Normal modes in an orthorhombic medium

Yuriy Ivanov* and Alexey Stovas

IGP, NTNU

April 23rd, 2018
RoSe meeting

Outline

Normal modes

Normal modes?

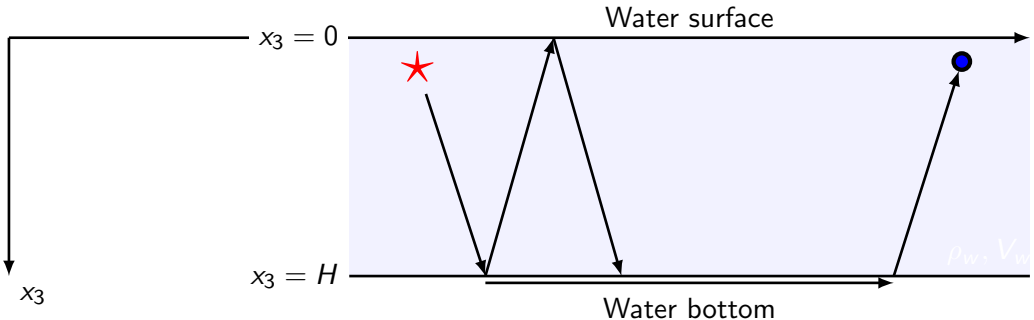

Figure 1: Sketch of a guided wave propagation. Vertical scale exaggerated.

Normal modes!

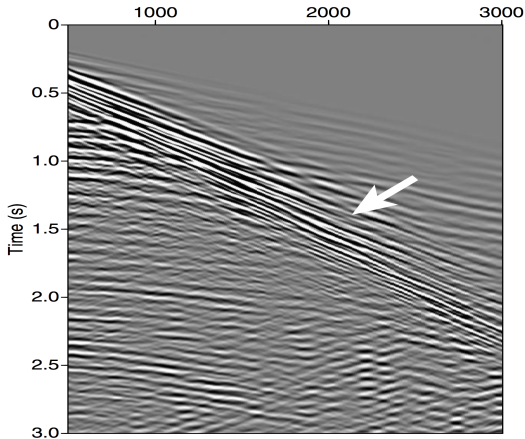

Figure 2: Typical marine common-shot gather (Wang et al., 2016).

Normal modes

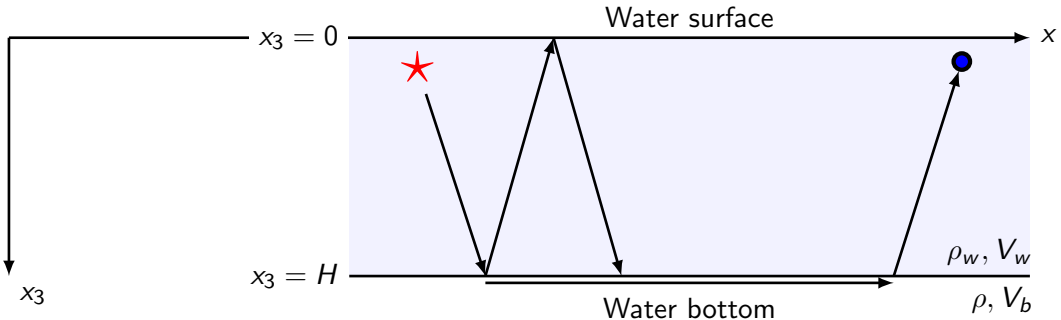

Figure 3: Sketch of a guided wave propagation. Vertical scale exaggerated.

Normal modes

Period equation: phase velocity

Acoustic case[1]:

$$\tan kH\sqrt{\frac{c^2}{V_w^2}-1}=-\frac{\rho}{\rho_w}\frac{\sqrt{\frac{c^2}{V_w^2}-1}}{\sqrt{1-\frac{c^2}{V_b^2}}}, \tag{1}$$

[1] Pekeris (1948); Press and Ewing (1950); Landrø and Hatchell (2012)

Normal modes

Period equation: phase velocity

Acoustic case[1]:

$$\tan kH\sqrt{\frac{c^2}{V_w^2}-1}=-\frac{\rho}{\rho_w}\frac{\sqrt{\frac{c^2}{V_w^2}-1}}{\sqrt{1-\frac{c^2}{V_b^2}}}, \tag{1}$$

where $k=\omega c^{-1}$.

[1] Pekeris (1948); Press and Ewing (1950); Landrø and Hatchell (2012)

Normal modes

Period equation: phase velocity

Acoustic case[1]:

$$\tan kH\sqrt{\frac{c^2}{V_w^2}-1}=-\frac{\rho}{\rho_w}\frac{\sqrt{\frac{c^2}{V_w^2}-1}}{\sqrt{1-\frac{c^2}{V_b^2}}}, \tag{1}$$

where $k=\omega c^{-1}$.

$$\boxed{c=c(\omega).}$$

[1] Pekeris (1948); Press and Ewing (1950); Landrø and Hatchell (2012)

Normal modes

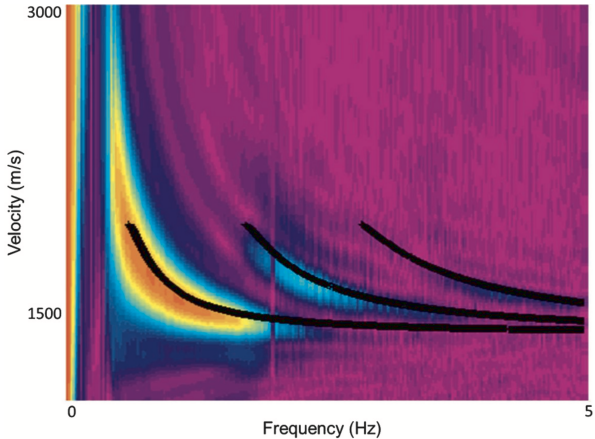

Figure 4: Estimated phase velocity dispersion curves (Hatchell and Mehta, 2010).

Normal modes

Period equation: group velocity

Group (envelope or modulation) velocity:

$$U = \frac{d\omega}{dk}, \tag{2}$$

Normal modes

Period equation: group velocity

Group (envelope or modulation) velocity:

$$U = \frac{d\omega}{dk}, \tag{2}$$

Solving the period equation (5),

$$\boxed{U = U(\omega).}$$

Normal modes

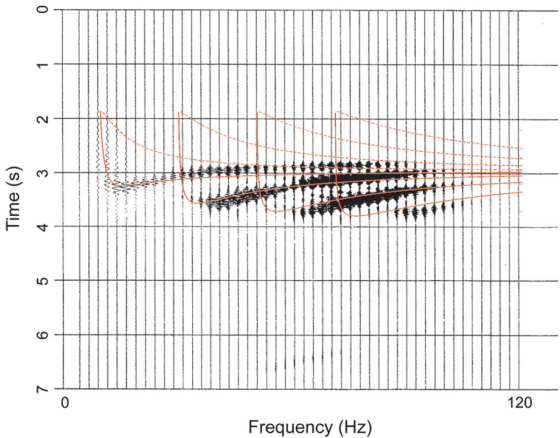

Figure 5: Frequency analysis: group and phase velocity dispersion (Landrø and Hatchell, 2012).

Normal modes

Signal or noise?

- Shallow marine sediments characterization,

Normal modes

Signal or noise?

- Shallow marine sediments characterization,
- Better denoising.

Orthorhombic media

Orthorhombic media?

- Anisotropic symmetry class,

Orthorhombic media?

- Anisotropic symmetry class,
  $\rightarrow$ $V = V(\alpha, \theta)$,

Orthorhombic media?

- Anisotropic symmetry class,
  - $\rightarrow$ $V = V(\alpha, \theta)$,
  - $\rightarrow$ 1x P-wave, 2x S-waves,

Orthorhombic media?

- Anisotropic symmetry class,
  - $\rightarrow$ $V = V(\alpha, \theta)$,
  - $\rightarrow$ 1x P-wave, 2x S-waves,
- Three mutually orthogonal planes of mirror symmetry,

Orthorhombic media?

- Anisotropic symmetry class,
  - $\rightarrow$ $V = V(\alpha, \theta)$,
  - $\rightarrow$ 1x P-wave, 2x S-waves,
- Three mutually orthogonal planes of mirror symmetry,
- 9 (nine) independent parameters + density,

Orthorhombic media?

- Anisotropic symmetry class,
  - $\rightarrow$ $V = V(\alpha, \theta)$,
  - $\rightarrow$ 1x P-wave, 2x S-waves,
- Three mutually orthogonal planes of mirror symmetry,
- 9 (nine) independent parameters + density,
- Suitable for description of fractured (and layered) rocks.

Orthorhombic media!

Figure 6: Fractured sandstone: orthorhombic symmetry.

Orthorhombic media

Hooke's law

$$\boldsymbol{\sigma} = \boldsymbol{c}\boldsymbol{\epsilon}, \tag{3}$$

Orthorhombic media

Hooke's law

$$\boldsymbol{\sigma} = \boldsymbol{c}\boldsymbol{\epsilon}, \tag{3}$$

stress tensor

Orthorhombic media

Hooke's law

$$\boldsymbol{\sigma} = \boldsymbol{c}\boldsymbol{\epsilon}, \tag{3}$$

stress tensor strain tensor

Orthorhombic media

Hooke's law

$$\boldsymbol{\sigma} = \boldsymbol{c}\boldsymbol{\epsilon}, \tag{3}$$

stress tensor strain tensor stiffness tensor

Orthorhombic media

Stiffness tensor

$$\mathbf{C} = \begin{pmatrix} c_{11} & c_{12} & c_{13} & & & \\ & c_{22} & c_{23} & & & \\ & & c_{33} & & & \\ & \text{SYM} & & c_{44} & & \\ & & & & c_{55} & \\ & & & & & c_{66} \end{pmatrix}. \tag{4}$$

Normal modes in orthorhombic media

Motivation

- A classical problem with a practical potential:

Motivation

- A classical problem with a practical potential:
- VTI is a feasible model[2],

[2] Landrø and Hatchell (2012); Skopintseva et al. (2013)

Motivation

- A classical problem with a practical potential:
- VTI is a feasible model[2],
- Sub-vertical fractures in gas-hydrate bearing sediments[3],

[2] Landrø and Hatchell (2012); Skopintseva et al. (2013)
[3] Lee and Collett (2009); Cook et al. (2010)

Motivation

- A classical problem with a practical potential:
- VTI is a feasible model[2],
- Sub-vertical fractures in gas-hydrate bearing sediments[3],
- Intersecting fracture systems[4],

[2] Landrø and Hatchell (2012); Skopintseva et al. (2013)
[3] Lee and Collett (2009); Cook et al. (2010)
[4] Sriram et al. (2013)

Motivation

- A classical problem with a practical potential:
- VTI is a feasible model[2],
- Sub-vertical fractures in gas-hydrate bearing sediments[3],
- Intersecting fracture systems[4],
- 15% azimuthal anisotropy[5].

[2] Landrø and Hatchell (2012); Skopintseva et al. (2013)
[3] Lee and Collett (2009); Cook et al. (2010)
[4] Sriram et al. (2013)
[5] Kumar et al. (2006)

Normal modes

Acoustic case

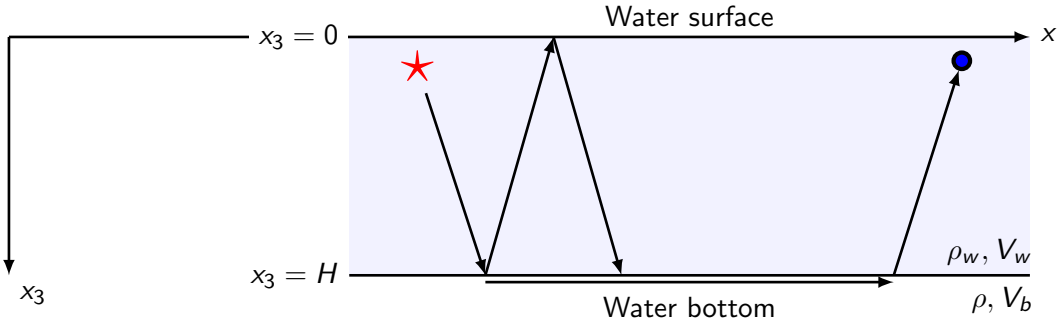

Figure 7: Sketch of a guided wave propagation. Vertical scale exaggerated.

Normal modes

Orthorhombic case

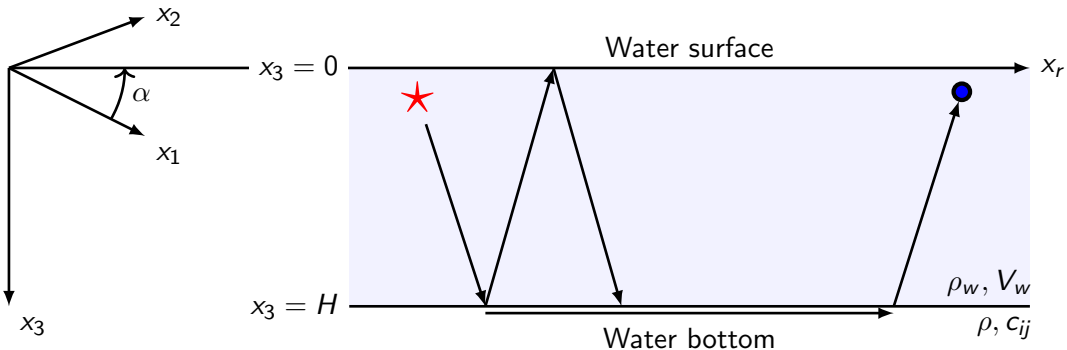

Figure 8: Sketch of a guided wave propagation. Vertical scale exaggerated.

Period equation

Elastic orthorhombic media: phase velocity

Ivanov and Stovas (2017):

$$\tan k_r H \sqrt{\frac{c^2}{V_w^2} - 1} = \frac{\sqrt{\frac{c^2}{V_w^2} - 1}}{c^2 \rho_w} \left(\rho c^2 - c_{44} \sin\alpha^2 - c_{55} \cos\alpha^2\right) \times \frac{c_{13} \cos\alpha^2 + c_{23} \sin\alpha^2 + \rho c^2 - c_{33}(\nu_1\nu_3 + \nu_2\nu_3 + \nu_1\nu_2)}{(\nu_1 + \nu_2 + \nu_3)\left(\rho c^2 - c_{44} \sin^2\alpha - c_{55} \cos^2\alpha\right) - c_{33}\nu_1\nu_2\nu_3}. \quad (5)$$

Period equation

Elastic orthorhombic media: phase velocity

Ivanov and Stovas (2017):

$$\tan k_r H \sqrt{\frac{c^2}{V_w^2} - 1} = \frac{\sqrt{\frac{c^2}{V_w^2} - 1}}{c^2 \rho_w} \left(\rho c^2 - c_{44} \sin\alpha^2 - c_{55} \cos\alpha^2\right) \times \frac{c_{13} \cos\alpha^2 + c_{23} \sin\alpha^2 + \rho c^2 - c_{33}(\nu_1\nu_3 + \nu_2\nu_3 + \nu_1\nu_2)}{(\nu_1 + \nu_2 + \nu_3)\left(\rho c^2 - c_{44} \sin^2\alpha - c_{55} \cos^2\alpha\right) - c_{33}\nu_1\nu_2\nu_3}. \quad (5)$$

radial wavenumber

Period equation

Elastic orthorhombic media: phase velocity

Ivanov and Stovas (2017):

$$\tan k_r H \sqrt{\frac{c^2}{V_w^2} - 1} = \frac{\sqrt{\frac{c^2}{V_w^2} - 1}}{c^2 \rho_w} \left(\rho c^2 - c_{44} \sin\alpha^2 - c_{55} \cos\alpha^2\right) \times \frac{c_{13} \cos\alpha^2 + c_{23} \sin\alpha^2 + \rho c^2 - c_{33}(\nu_1\nu_3 + \nu_2\nu_3 + \nu_1\nu_2)}{(\nu_1 + \nu_2 + \nu_3)\left(\rho c^2 - c_{44} \sin^2\alpha - c_{55} \cos^2\alpha\right) - c_{33}\nu_1\nu_2\nu_3}. \quad (5)$$

radial wavenumber phase azimuth

Period equation

Elastic orthorhombic media: phase velocity

Ivanov and Stovas (2017):

$$\tan k_r H \sqrt{\frac{c^2}{V_w^2} - 1} = \frac{\sqrt{\frac{c^2}{V_w^2} - 1}}{c^2 \rho_w} \left(\rho c^2 - c_{44} \sin\alpha^2 - c_{55} \cos\alpha^2\right) \times \frac{c_{13} \cos\alpha^2 + c_{23} \sin\alpha^2 + \rho c^2 - c_{33}(\nu_1\nu_3 + \nu_2\nu_3 + \nu_1\nu_2)}{(\nu_1 + \nu_2 + \nu_3)\left(\rho c^2 - c_{44} \sin^2\alpha - c_{55} \cos^2\alpha\right) - c_{33}\nu_1\nu_2\nu_3}. \quad (5)$$

radial wavenumber phase azimuth P/S1/S2-waves attenuation coefficients

Numerical example

Model

$$\mathbf{C} = \begin{pmatrix} 9 & 2.25 & 3.6 & & & \\ & 5.94 & 2.4 & & & \\ & & 9.84 & 0 & & \\ & \text{SYM} & & 2 & & \\ & & & & 2.182 & \\ & & & & & 1.6 \end{pmatrix}. \tag{6}$$

$\rho/\rho_w = 1.56$, $V_w = 1.485$ km s^{-1}, $H = 0.075$ km.

Numerical example

Dispersion curves

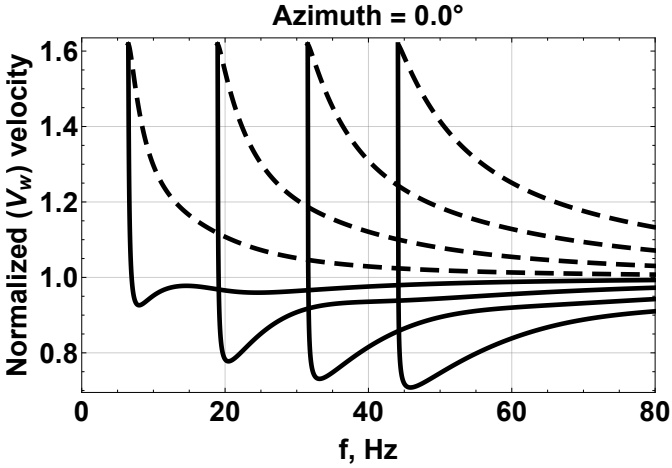

Figure 9: Phase (- - -) and group (——) velocities.

Numerical example

Dispersion curves

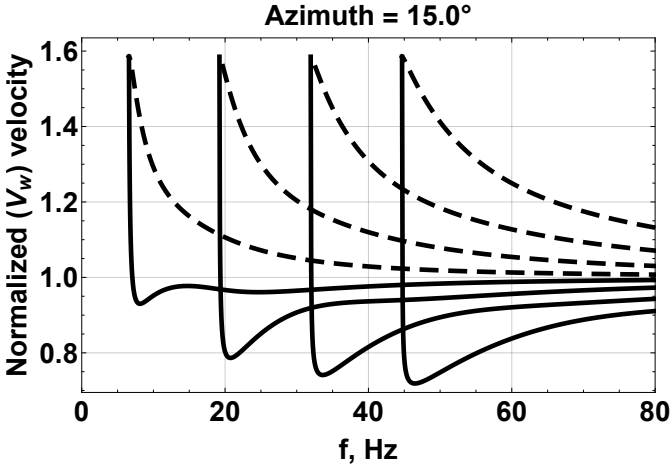

Figure 9: Phase (- - -) and group (——) velocities.

Numerical example

Dispersion curves

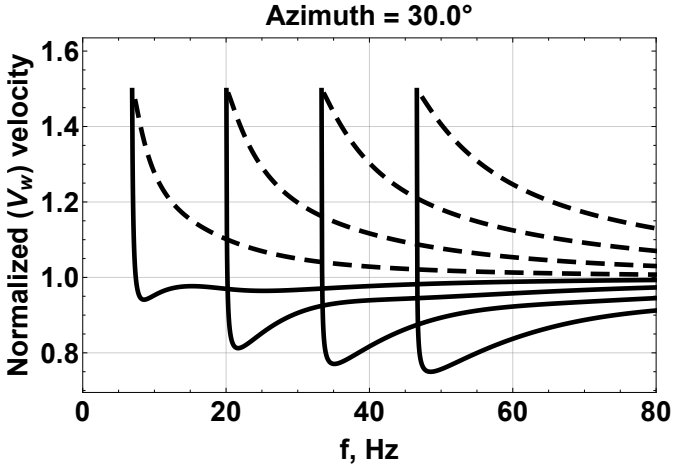

Figure 9: Phase (- - -) and group (——) velocities.

Numerical example

Dispersion curves

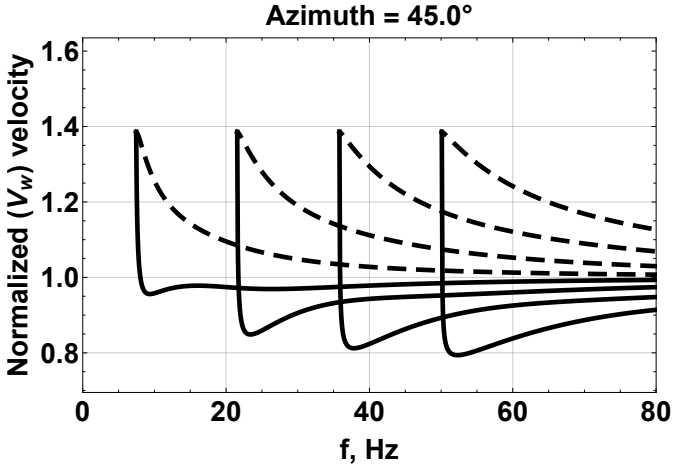

Figure 9: Phase (- - -) and group (——) velocities.

Numerical example

Dispersion curves

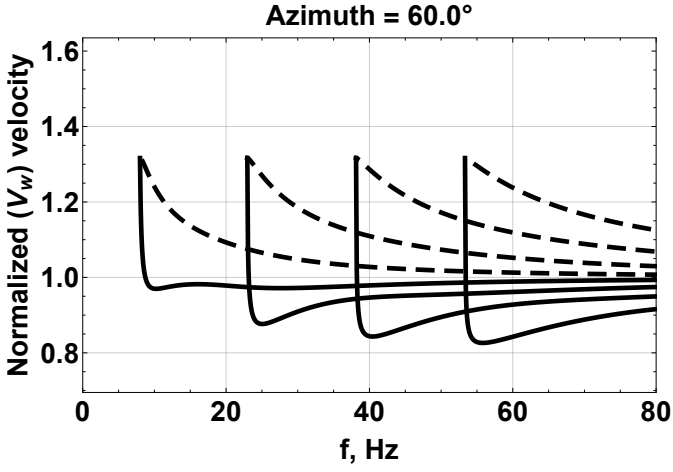

Figure 9: Phase (- - -) and group (——) velocities.

Numerical example

Dispersion curves

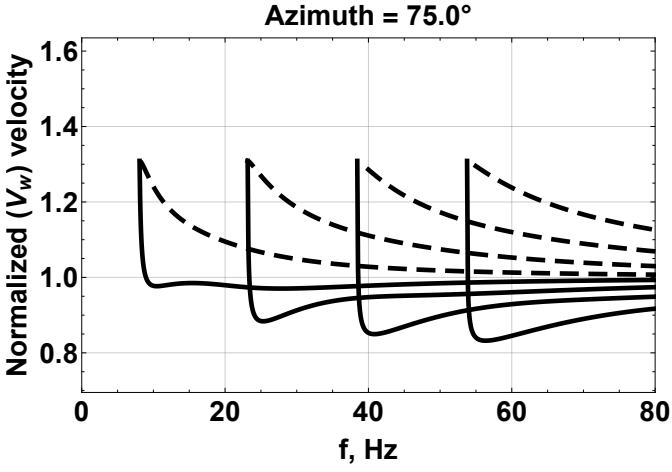

Figure 9: Phase (- - -) and group (——) velocities.

Numerical example

Dispersion curves

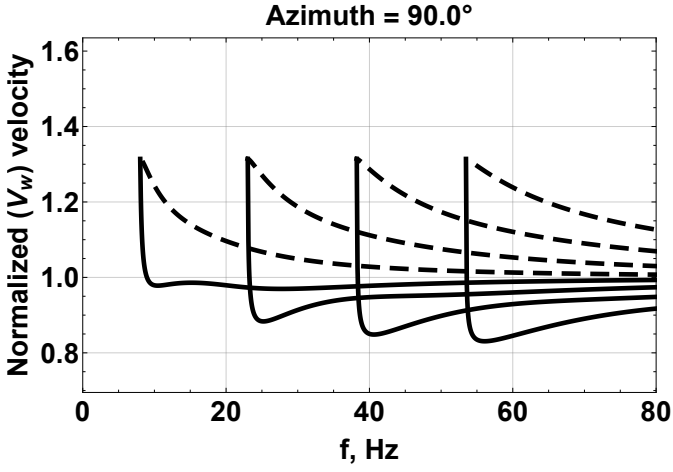

Figure 9: Phase (- - -) and group (——) velocities.

Period equation

Elastic orthorhombic media: group velocity

Group velocity vector:

$$\mathbf{U} = \frac{d\omega}{d\mathbf{k}} \tag{7}$$

Period equation

Elastic orthorhombic media: group velocity

Group velocity vector:

$$\mathbf{U} = \frac{d\omega}{d\mathbf{k}} = \{U_r, U_\alpha\}, \tag{7}$$

Period equation

Elastic orthorhombic media: group velocity

Group velocity vector:

$$\mathbf{U} = \frac{d\omega}{d\mathbf{k}} = \{U_r, U_\alpha\}, \tag{7}$$

Steering angle:

$$\beta = \tan^{-1} \frac{U_\alpha}{U_r}, \tag{8}$$

Period equation

Elastic orthorhombic media: group velocity

Group velocity vector:

$$\mathbf{U} = \frac{d\omega}{d\mathbf{k}} = \{U_r, U_\alpha\}, \tag{7}$$

Steering angle:

$$\beta = \tan^{-1} \frac{U_\alpha}{U_r}, \tag{8}$$

Group azimuth:

$$\phi = \alpha + \beta. \tag{9}$$

Period equation

Group velocity

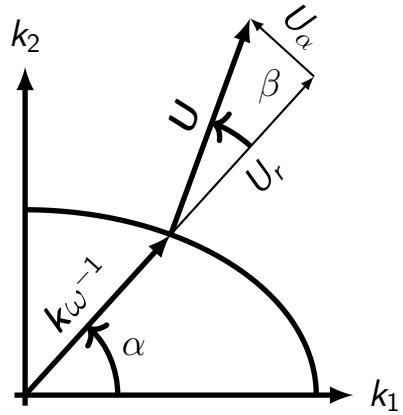

Figure 10: Schematic of the phase and group velocity vectors relation (horizontal plane).

Numerical example

Numerical example

Dispersion curves

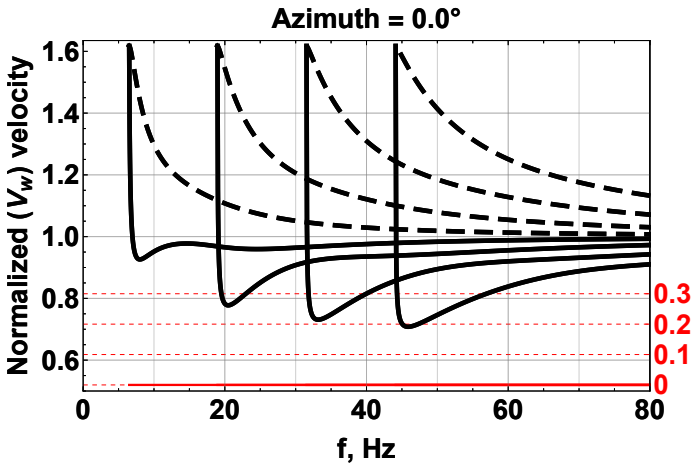

Figure 11: Phase (- - -), radial group (——), and tangential group velocities.

Numerical example

Dispersion curves

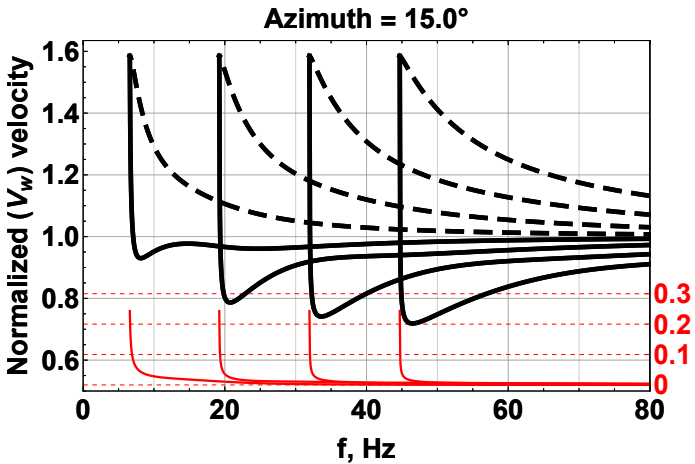

Figure 11: Phase (- - -), radial group (——), and tangential group velocities.

Numerical example

Dispersion curves

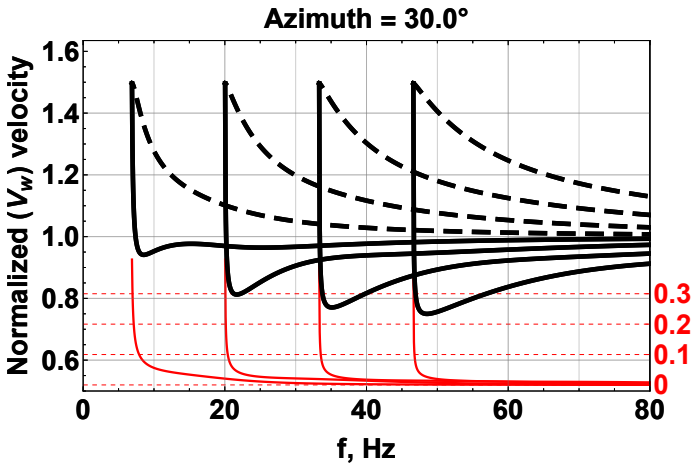

Figure 11: Phase (- - -), radial group (——), and tangential group velocities.

Numerical example

Dispersion curves

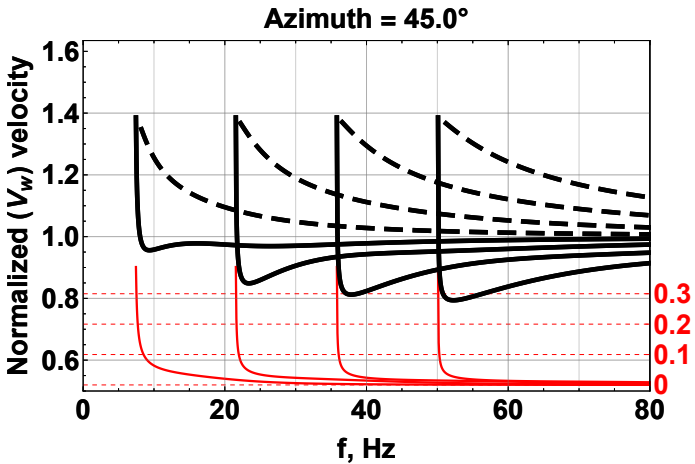

Figure 11: Phase (- - -), radial group (——), and tangential group velocities.

Numerical example

Dispersion curves

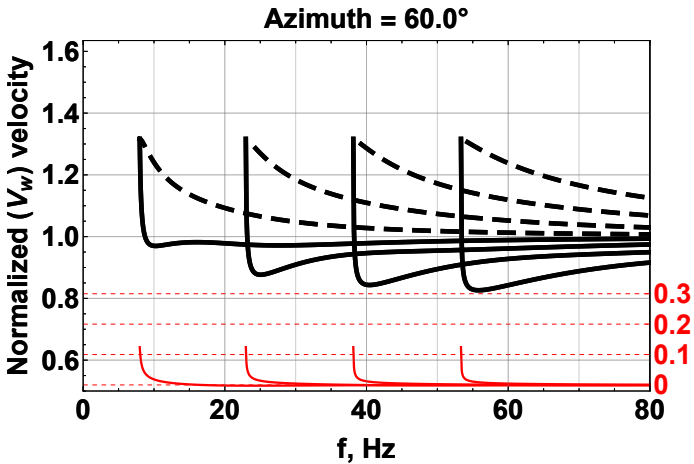

Figure 11: Phase (- - -), radial group (——), and tangential group velocities.

Numerical example

Dispersion curves

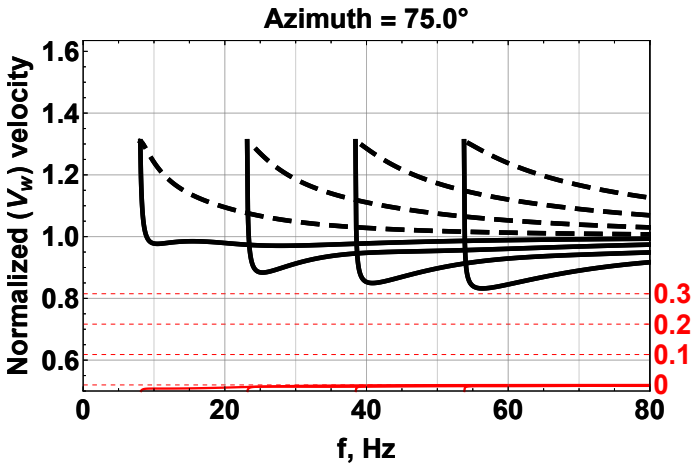

Figure 11: Phase (- - -), radial group (——), and tangential group velocities.

Numerical example

Dispersion curves

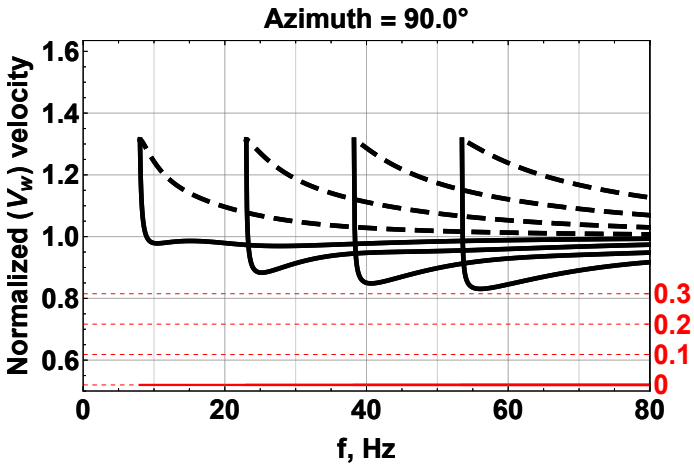

Figure 11: Phase (- - -), radial group (——), and tangential group velocities.

Numerical example

Azimuthal dependence

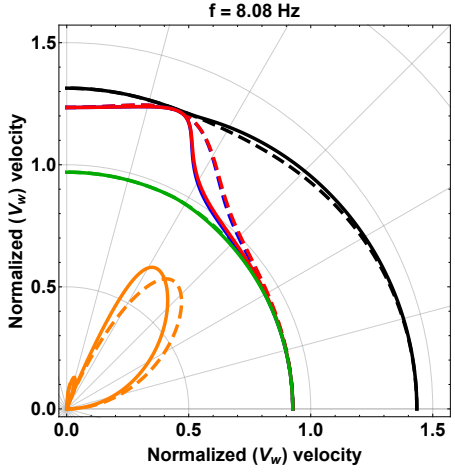

Figure 12: Azimuthal (α: - - -, ϕ: ——) dependence: c, U_r, $|\boldsymbol{U}|$, $U_\alpha \times 5$, $\min_\omega U_r$.

Numerical example

Azimuthal dependence

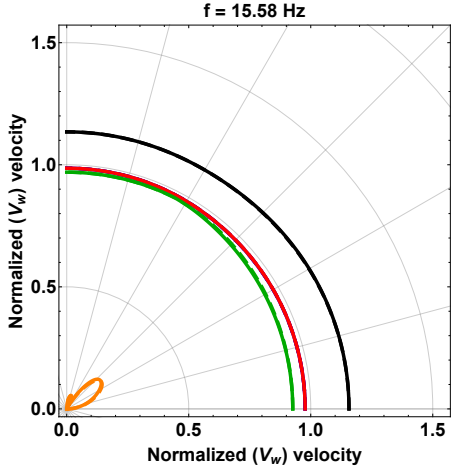

Figure 12: Azimuthal (α: - - -, ϕ: ——) dependence: c, U_r, $|\boldsymbol{U}|$, $U_\alpha \times 5$, $\min_\omega U_r$.

Numerical example

Azimuthal dependence

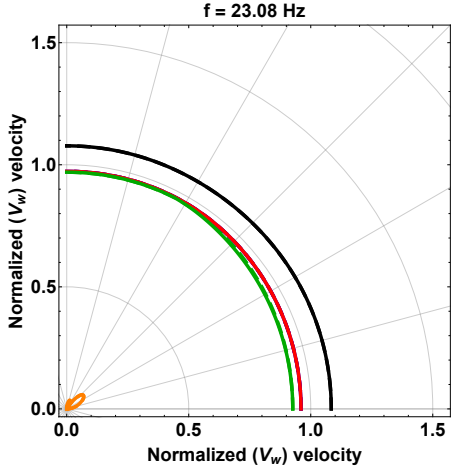

Figure 12: Azimuthal (α: - - -, ϕ: ——) dependence: c, U_r, $|\boldsymbol{U}|$, $U_\alpha \times 5$, $\min_\omega U_r$.

Numerical example

Azimuthal dependence

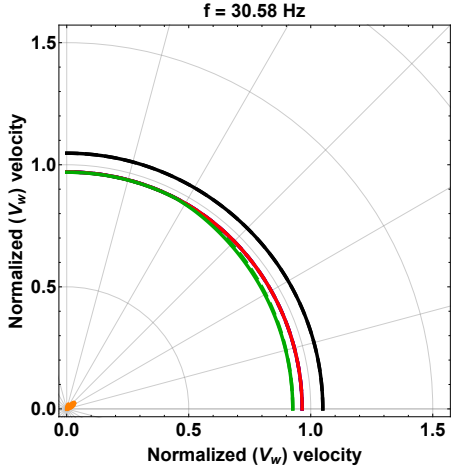

Figure 12: Azimuthal (α: - - -, ϕ: ——) dependence: c, U_r, $|\boldsymbol{U}|$, $U_\alpha \times 5$, $\min_\omega U_r$.

Numerical example

Azimuthal dependence

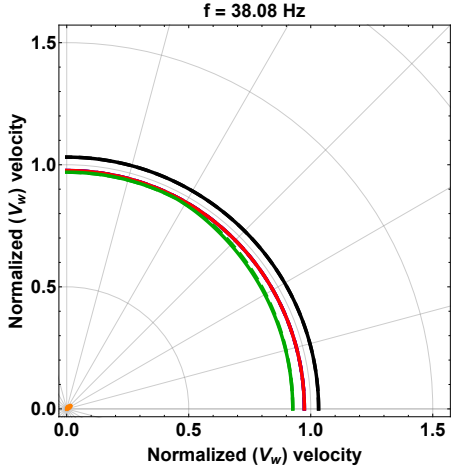

Figure 12: Azimuthal (α: - - -, ϕ: ——) dependence: c, U_r, $|\boldsymbol{U}|$, $U_\alpha \times 5$, $\min_\omega U_r$.

Numerical example

Azimuthal dependence

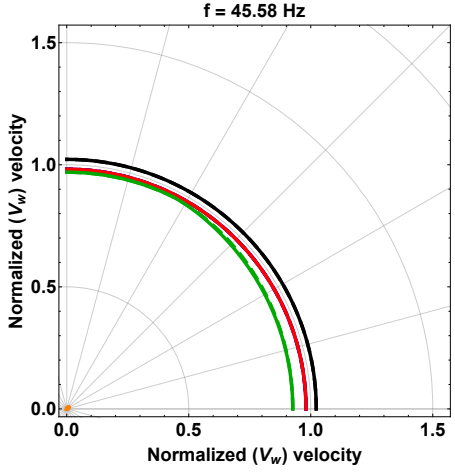

Figure 12: Azimuthal (α: - - -, ϕ: ——) dependence: c, U_r, $|\boldsymbol{U}|$, $U_\alpha \times 5$, $\min_\omega U_r$.

Numerical example

Azimuthal dependence

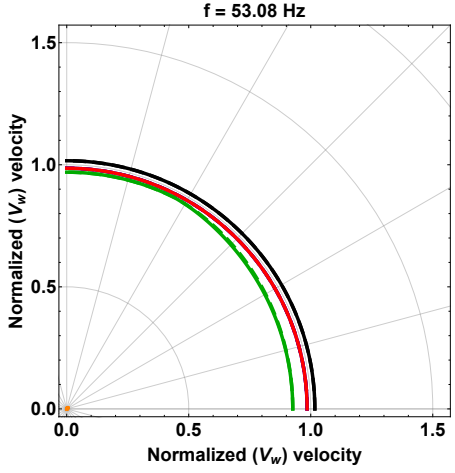

Figure 12: Azimuthal (α: - - -, ϕ: ——) dependence: c, U_r, $|\boldsymbol{U}|$, $U_\alpha \times 5$, $\min_\omega U_r$.

Numerical example

Azimuthal dependence

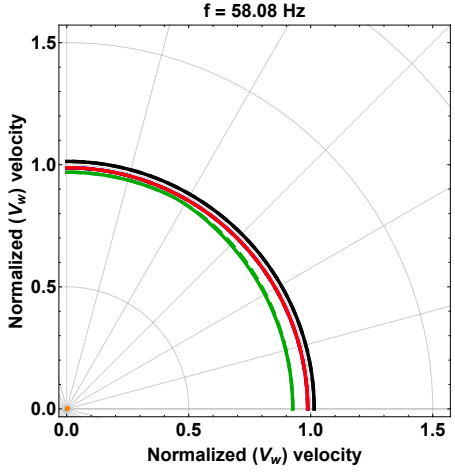

Figure 12: Azimuthal (α: - - -, ϕ: ——) dependence: c, U_r, $|\boldsymbol{U}|$, $U_\alpha \times 5$, $\min_\omega U_r$.

Numerical example

Azimuthal dependence

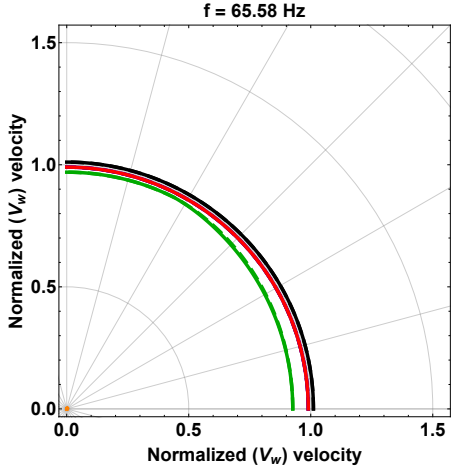

Figure 12: Azimuthal (α: - - -, ϕ: ——) dependence: c, U_r, $|\boldsymbol{U}|$, $U_\alpha \times 5$, $\min_\omega U_r$.

Numerical example

Azimuthal dependence

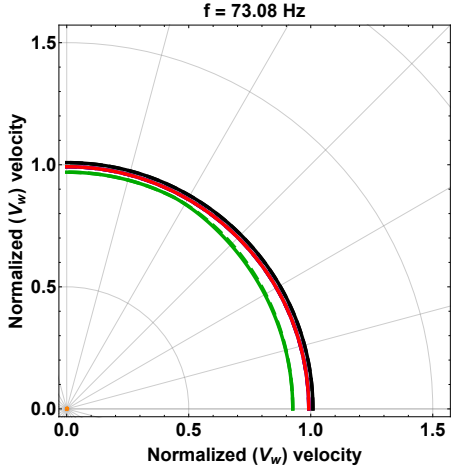

Figure 12: Azimuthal (α: - - -, ϕ: ——) dependence: c, U_r, $|\boldsymbol{U}|$, $U_\alpha \times 5$, $\min_\omega U_r$.

Numerical example

Azimuthal dependence

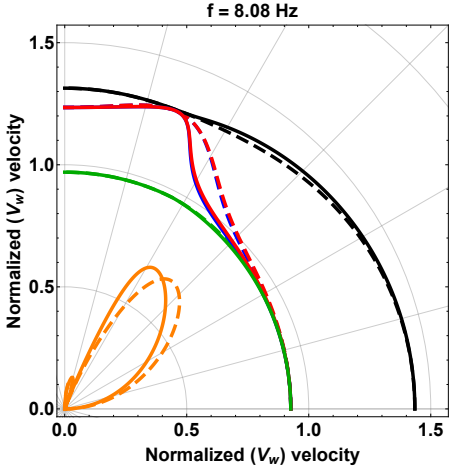

Figure 13: Azimuthal (α: - - -, ϕ: ——) dependence: c, U_r, $|\boldsymbol{U}|$, $U_\alpha \times 5$, $\min_\omega U_r$.

Numerical example

Azimuthal dependence

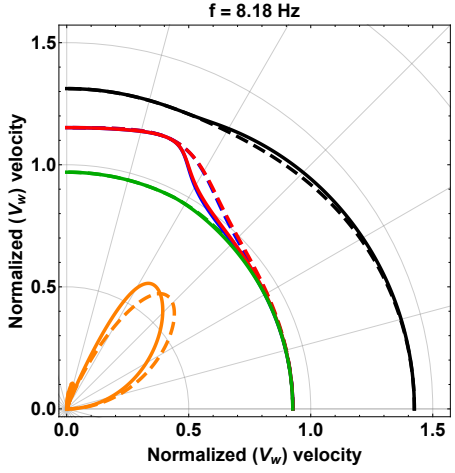

Figure 13: Azimuthal (α: - - -, ϕ: ——) dependence: c, U_r, $|\boldsymbol{U}|$, $U_\alpha \times 5$, $\min_\omega U_r$.

Numerical example

Azimuthal dependence

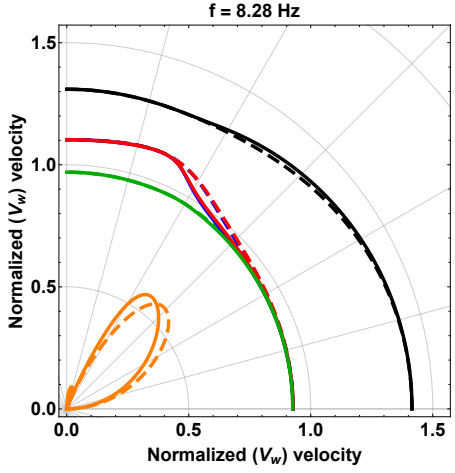

Figure 13: Azimuthal (α: - - -, ϕ: ——) dependence: c, U_r, $|\boldsymbol{U}|$, $U_\alpha \times 5$, $\min_\omega U_r$.

Numerical example

Azimuthal dependence

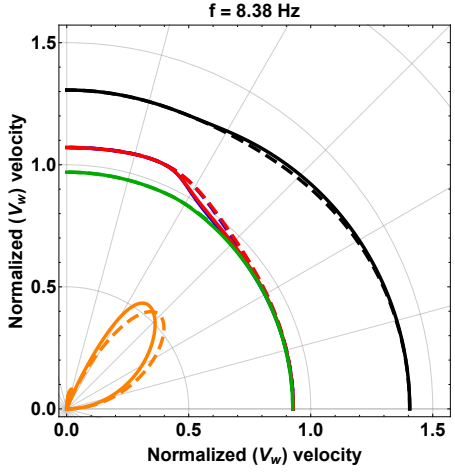

Figure 13: Azimuthal (α: - - -, ϕ: ——) dependence: c, U_r, $|\boldsymbol{U}|$, $U_\alpha \times 5$, $\min_\omega U_r$.

Numerical example

Azimuthal dependence

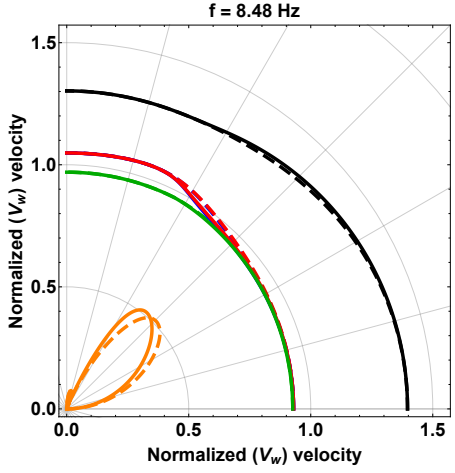

Figure 13: Azimuthal (α: - - -, ϕ: ——) dependence: c, U_r, $|\boldsymbol{U}|$, $U_\alpha \times 5$, $\min_\omega U_r$.

Numerical example

Azimuthal dependence

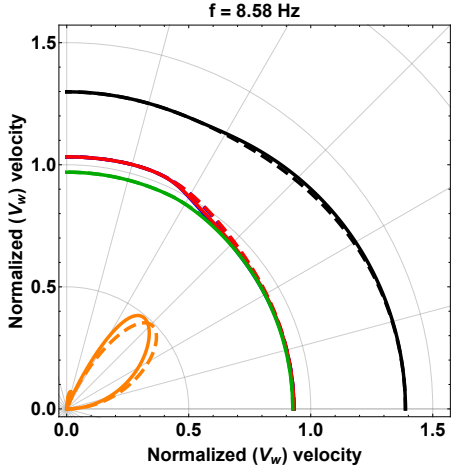

Figure 13: Azimuthal (α: - - -, ϕ: ——) dependence: c, U_r, $|\boldsymbol{U}|$, $U_\alpha \times 5$, $\min_\omega U_r$.

Numerical example

Azimuthal dependence

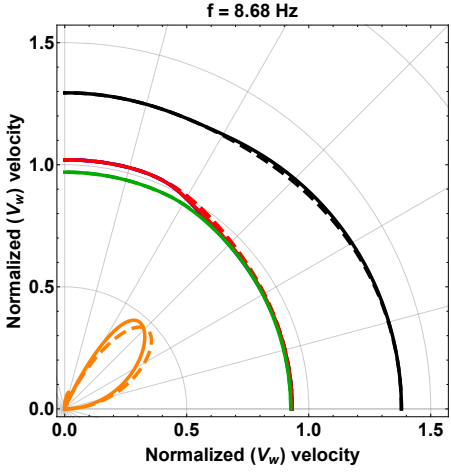

Figure 13: Azimuthal (α: - - -, ϕ: ——) dependence: c, U_r, $|\boldsymbol{U}|$, $U_\alpha \times 5$, $\min_\omega U_r$.

Numerical example

Azimuthal dependence

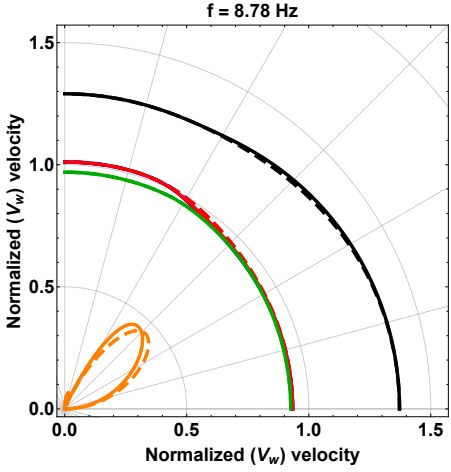

Figure 13: Azimuthal (α: - - -, ϕ: ——) dependence: c, U_r, $|\boldsymbol{U}|$, $U_\alpha \times 5$, $\min_\omega U_r$.

Numerical example

Azimuthal dependence

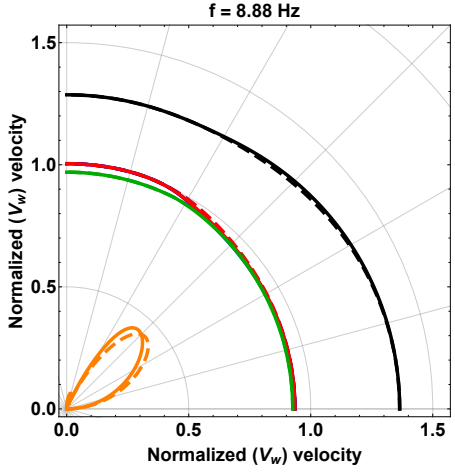

Figure 13: Azimuthal (α: - - -, ϕ: ——) dependence: c, U_r, $|\boldsymbol{U}|$, $U_\alpha \times 5$, $\min_\omega U_r$.

Numerical example

Azimuthal dependence

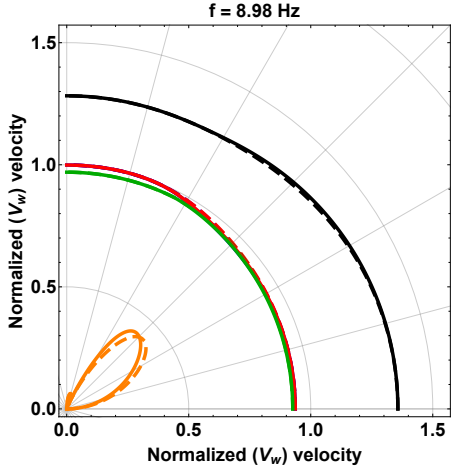

Figure 13: Azimuthal (α: - - -, ϕ: ——) dependence: c, U_r, $|\boldsymbol{U}|$, $U_\alpha \times 5$, $\min_\omega U_r$.

Numerical example

Dispersion curves

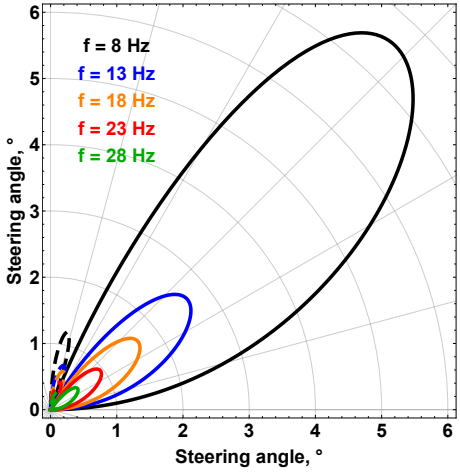

Figure 14: Steering angle.

Useful simplification

Orthorhombic media

Stiffness tensor

$$\mathbf{C} = \begin{pmatrix} c_{11} & c_{12} & c_{13} & & & \\ & c_{22} & c_{23} & & & \\ & & c_{33} & & & \\ & \text{SYM} & & c_{44} & & \\ & & & & c_{55} & \\ & & & & & c_{66} \end{pmatrix}. \tag{10}$$

Ellipsoidal orthorhombic media

Stiffness tensor

$$\mathbf{C} = \rho \begin{pmatrix} V_1^2 & V_1 V_2 & V_1 V_3 & & & \\ & V_2^2 & V_1 V_2 & & & \\ & & V_3^2 & & & \\ & \text{SYM} & & 0 & & \\ & & & & 0 & \\ & & & & & 0 \end{pmatrix}. \qquad (11)$$

Ellipsoidal orthorhombic media

Period equation

$$\tan k_r H \sqrt{\frac{c^2}{V_w^2} - 1} = -\frac{\rho}{\rho_w} \frac{\sqrt{\frac{c^2}{V_w^2} - 1}}{\sqrt{\frac{V_2^2 \sin^2\alpha + V_1^2 \cos^2\alpha}{V_3^2} - \frac{c^2}{V_3^2}}}. \tag{12}$$

Acoustic media

Period equation

$$\tan kH\sqrt{\frac{c^2}{V_w^2}-1}=-\frac{\rho}{\rho_w}\frac{\sqrt{\frac{c^2}{V_w^2}-1}}{\sqrt{1-\frac{c^2}{V_b^2}}}. \tag{13}$$

Ellipsoidal orthorhombic media

Group-velocity limits

$$\{U_r, U_\alpha\}|_{\omega\to\infty} = \{V_w, 0\}\,,$$

Ellipsoidal orthorhombic media

Group-velocity limits

$$\{U_r, U_\alpha\}|_{\omega\to\infty} = \{V_w, 0\}\,,$$

$$\{U_r, U_\alpha\}|_{\omega\to\omega_{\text{cut-off}}} = \left\{\sqrt{V_2^2\sin^2\alpha + V_1^2\cos^2\alpha},\, \frac{\left(V_1^2 - V_2^2\right)\sin\alpha\cos\alpha}{\sqrt{V_2^2\sin^2\alpha + V_1^2\cos^2\alpha}}\right\}, \tag{14}$$

Conclusions

- Period equation in orthorhombic media,

Conclusions

- Period equation in orthorhombic media,
- Ellipsoidal approximation,

Conclusions

- Period equation in orthorhombic media,
- Ellipsoidal approximation,
- Group velocity vector,

Conclusions

- Period equation in orthorhombic media,
- Ellipsoidal approximation,
- Group velocity vector,
- Potential use for water-bottom sediments characterization.

Acknowledgments

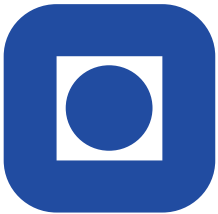

Acknowledgments

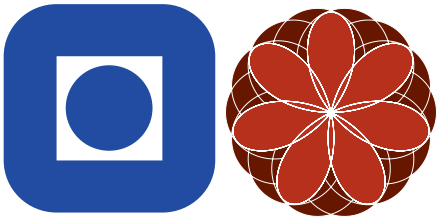

Acknowledgments

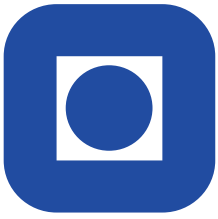
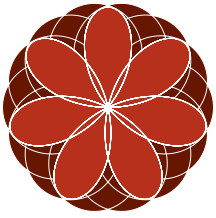
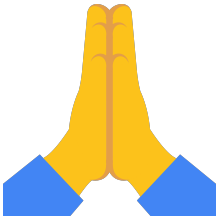

References I

Cook, A., B. Anderson, A. Malinverno, S. Mrozewski, and D. Goldberg, 2010, Electrical anisotropy due to gas hydrate-filled fractures: Geophysics, **75**, F173–F185.

Hatchell, P., and K. Mehta, 2010, Ocean Bottom Seismic (OBS) timing drift correction using passive seismic data: 80th Annual International Meeting, SEG, Expanded Abstracts, 2054–2058.

Ivanov, Y., and A. Stovas, 2017, Normal Modes in Orthorhombic Media: 79th EAGE Conference and Exhibition, EAGE, Extended Abstracts, We P6 03.

Kumar, D., M. K. Sen, N. L. Bangs, C. Wang, and I. Pecher, 2006, Seismic anisotropy at Hydrate Ridge: Geophysical Research Letters, **33**, L01306.

Landrø, M., and P. Hatchell, 2012, Normal modes in seismic data — Revisited: Geophysics, **77**, W27–W40.

Lee, M. W., and T. S. Collett, 2009, Gas hydrate saturations estimated from fractured reservoir at Site NGHP-01-10, Krishna-Godavari Basin, India: Journal of Geophysical Research: Solid Earth, **114**, B07102.

Pekeris, C. L., 1948, Theory of Propagation of Explosive Sound in Shallow Water: Geological Society of America Memoirs, **27**, 1–116.

Press, F., and M. Ewing, 1950, Propagation of explosive sound in a liquid layer overlying a semi-infinite elastic solid: Geophysics, **15**, 426–446.

References II

Skopintseva, L. V., M. Landrø, and A. Stovas, 2013, Normal Modes in Anisotropic VTI Media: 75th EAGE Conference and Exhibition, Th P03 07.

Sriram, G., P. Dewangan, T. Ramprasad, and P. Rama Rao, 2013, Anisotropic amplitude variation of the bottom-simulating reflector beneath fracture-filled gas hydrate deposit: Journal of Geophysical Research: Solid Earth, **118**, 2258–2274.

Wang, J., R. Stewart, N. Dyaur, and M. Bell, 2016, Marine guided waves: Subbottom property estimation and filtering using physical modeling data: Geophysics, **81**, V303–V315.